International Journal of Water Resources and Arid Environments 9(1): 56-70, 2020
ISSN 2079-7079

Integration of Raster Based Irrigation and Groundwater for Water Management in Punjab, Pakistan: a Modeling & GIS Based Approach

[1]Fahad Ejaz, [2]Catalin Stefan, [2]Aybulat Fatkhutdinov and [3]Muhammad Usman

[1]Stochastic Simulation and Safety Research for Hydrosystems, University of Stuttgart, Stuttgart, Germany
[2]Junior Research Group INOWAS, Technische Üniversität Dresden, Dresden, Germany
[3]Department of Irrigation & Drainage, University of Agriculture, Faisalabad, Pakistan

Abstract: In Pakistan, groundwater resources are depleting because of its unaccounted use for agricultural purposes. Its sustainable management will play a vital role in the socio-economic development which would be possible by developing a flexible groundwater modelling system which has the ability to incorporate all the natural processes responsible for groundwater dynamics. With this in mind, a Decision Support System (DSS) based on multi-source vector and raster data has been developed. Raster based groundwater simulations on monthly temporal resolutions have been carried out, which incorporates all the natural processes by using groundwater flow model (i.e. r.gwflow). The developed DSS is tested for two irrigation sub-divisions (Bhagat & Sultanpur) located in Rechna Doab, Punjab, Pakistan. Groundwater balance in the region has been analyzed for the recent cropping conditions and simulations were performed for different interventions in irrigation and cropping practices. The modeling results indicate that, maximum groundwater abstraction has been observed in the months of May and June, exceeding 250 Mm^3. Out of total crop consumptive water, 51% is fulfilled by canal water supply only. The best cropping practice with reference to maximum saving in groundwater resource is the cultivation of cotton, fodder (millet) during kharif cropping season and cultivation of wheat, fodder (oats, barley) during the rabi cropping season.

Key words: Evapotranspiration · Effective rainfall · Groundwater recharge · Groundwater extraction · Cropping pattern

INTRODUCTION

Majority of the fresh water resources of Pakistan have been exploited due to its overuse for variety of sectors like agriculture, domestic uses, industry and eco-environment [1]. The availability of fresh water for is shrinking for future generations [2]. Groundwater depletion has become an emerging issue in Pakistan from last few years which is quite prominent in irrigated Rechna Doab, that is an irrigated region located between rivers Ravi and Chenab.

Decision making for devising viable strategies of sustainable water use is guaranteed by the accurate estimation of water balance terms like evapotranspiration (ET), groundwater recharge, pumping and, groundwater inflow and outflow etc., [1]. A number of case studies have been conducted throughout the world which have interrogated the extent of problem both from the surface and groundwater point of view, adopting empirical, analytical and modeling techniques. The core information for all methods is crop evapotranspiration (ET_c) particularly for irrigated agricultural regions, which is calculated from the product of reference evapotranspiration (ET_o) and crop coefficients (K_c).

Et_o can be estimated with various techniques that require different climatological data types including temperature, wind speed, sun shine hours and relative humidity, for instance, Modified Penman method. Many other approaches (e.g., the Blaney-Criddle method and various empirical approaches) require less climatic data. The crop coefficients (K_c) can be estimated either with the so-called single crop coefficient method or the dual crop coefficient method, depending on the field conditions and type of irrigation [3]. Over the last few years, the Et_c

Corresponding Author: Fahad Ejaz, Stochastic Simulation and Safety Research for Hydrosystems, University of Stuttgart, Stuttgart, Germany. Tel: +49-17674719362, E-mail: fahad.ejaz@iws.uni-stuttgart.de.

estimating methods have been improved by the inclusion of different state of the art technologies including use of remote sensing data for estimation of different energy balance parameters for ET estimation [4]. ET_c is estimated by using the combination of dual crop coefficient approach with remotely-sensed data [5]. Surface Energy Balance Algorithm (SEBAL) is applied to estimate pixel-based ET_c values, using Moderate Resolution Imaging Spectroradiometer (MODIS) satellite images [1], [4]. [6] has used MODIS data for this purpose within the recent Calibration-free Evapotranspiration Mapping Technique (CREMAP) as devised by [7] can also be used [6]. The resulting evapotranspiration maps have been substantially improved.

The other important parameter is groundwater recharge which is often assessed separately from rest of the water budget. For instance, recharge estimation from rainfall with a cumulative rainfall departure method that require groundwater level information for validation [8]. Groundwater recharge can be estimated with a Darcian method based on pedotransfer functions and Chloride tracer data [9]. Water table fluctuation data is successfully used to estimate recharge from irrigation fields and rainfall [10]. Another technique used for estimating the time-dependent recharge resulting from seeping of branch canal system is through analytical models [11]. For a similar type of problem, different approaches of recharge estimation such as analytical, empirical and water balance methods have been compared [12, 13]. Recently, modern tools like remote sensing and GIS technology have been used for the evaluation of irrigation system in an agricultural area [14].

All water balance components are interconnected in a natural ecosystem, therefore, groundwater flow simulations using numerical approaches have often occurred to support water budget estimates with regionalization of water table, recharge rates and model-based estimates of other exchange fluxes. Acceptable groundwater pumping rates are estimated through numerical groundwater flow simulations [15]; estimation for gains and losses of streams and to analyze the impact of water transfer on nearby areas, the finite-difference flow simulations are used [16]. Whereas, groundwater flow simulations are used for regional behaviors of groundwater together with net groundwater recharge rates as obtained from the water balance method [17]. Flow simulations also appear in the already reported study by [1].

Under the situation of acute challenges faced by the groundwater sector in Pakistan, decision makers have to make decisions and strategic planning for its sustainable use. The two questions which need to be answered straightaway based on the concrete information are; (1) current water balance situation and how it would change with time; (2) actions which needs to be taken for sustainable use of groundwater. Therefore, the overall objective of this study was to develop an interactive system that integrates existing cropping information together with spatially distributed groundwater flow model. The organization of the current manuscript is that its first section describes the study area and data sources, second section discusses about the materials and adopted methods, while the third section demonstrates the detailed results of the present study.

Description of the Study Area

Location: Two irrigation subdivisions of Lower Chenab Canal (LCC), Punjab Pakistan, i.e., Bhagat and Sultanpur were chosen as a study area. The study area consist of 1581.7 square kilometers and geographical co-ordinates are 30°45?0' N 72°25?0' E at the center of territory. The study area is bounded on western side by Trimmu Sidhnai (T.S) link canal and on southern side with river Ravi. The T.S link canal brings water from river Chenab to the river Ravi. River Ravi is a transboundary river of India and Pakistan, origin of this river is in India. The area is a depositional plain which is a part of alluvium-filled Indo Gangetic plane. The elevation ranges from 141 to 174 m.a.s.l.

Hydrogeology: The study region is a part of enormous flood plain and unconfined aquifer is extended over the basin. The basement consists of metamorphic and igneous rocks of Precambrian age. The area is laid beneath highly stratified unconsolidated alluvial material which is composed of sand of various grades interbedded with discontinuous lenses of silt, clay and nodules of kanker (a calcium carbonate) of secondary origin deposited by present and ancestral tributaries of the Indus River [17]. Pumping tests and lithological mechanical analyses of test holes shows hydraulic conductivity in a range between 6.10E-04 to 3.05E-03 ms^{-1} and specific yield is in a range of 0.06 to 0.33 [18]. The test boreholes available in the study area shows four soil texture classes, i.e., sand, silt, clay and gravel. There is no typical pattern in the arrangement of these materials.

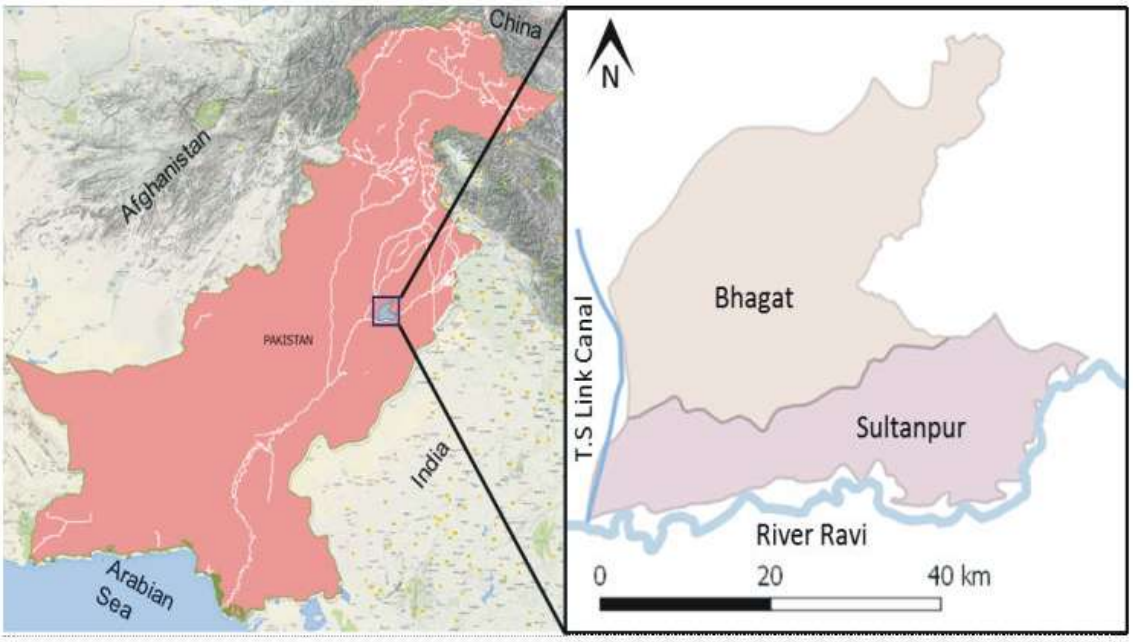

Fig. 1: Location of the Study Area

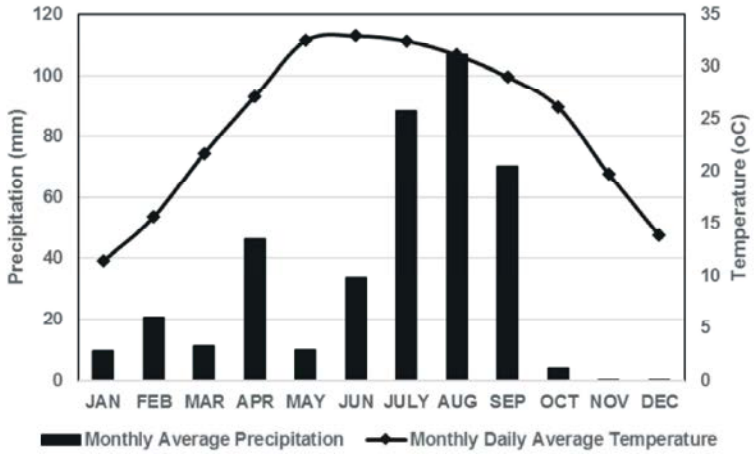

Fig. 2: Climograph representing monthly averaged precipitation and monthly daily averaged temperature for the period 2009-2011

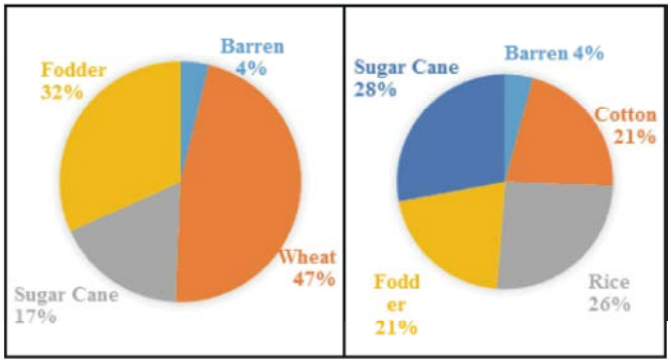

Fig. 3: Cropping pattern of the study area in Kharif (left) and Rabi (right) season

Table 1: Sources of data used for research

Data	Source
Digital Elevation Model (DEM)	Shuttle Radar Topography Mission (SRTM) http://www.srtm.csi.cgiar.org
Climatic variables	Pakistan Meteorological Department (PMD), Islamabad, Pakistan.
Piezometric water level	Salinity Monitoring Organization (SMO), WAPDA, Pakistan.
Bore logs data	International Water Management Institute (IWMI), Lahore Pakistan.
Canal flows data	Irrigation Department, Punjab Pakistan.
Shape files	Irrigation Department, Punjab Pakistan.

Climate & Cropping Practices: The climate in the study region is sub humid with hottest month of June with an average highest temperature of 42°C and average lowest temperature of 28°C. January is the coldest month with average lowest temperature of 5°C and average highest temperature of 21°C. About 255 mm of average annual precipitation fall out of which 70% occurs during the monsoon season (July to September).

There are two main cropping seasons, i.e., rabi and kharif cropping seasons. The kharif season usually starts from May and ends in October, whereas the time period for rabi season is from November to April. Different crops are cultivated throughout the year, rice, sugarcane, cotton and fodder (mainly sorghum, maize and millet) are grown in kharif season, while sugarcane, wheat and fodder (mainly barseem and oat) are grown in rabi season. Sugarcane is the annual crop and takes longer time (10-12 months) for growing as compared to other crops. Groundwater is used to fulfil a considerable part of crop water needs and it mainly comes from the seepage losses of canals and rainfall. The two irrigation subdivisions are located at the end of the Lower Chenab Canal (LCC East) irrigation system where reduced canal flow reaches to the farmlands.

Data Sources: A variety of data were utilized in accomplishing of the objectives of this study. The data have been acquired from different sources which includes satellite data as well as the ground observations. The relevant data and their sources are given as follows:

MATERIALS AND METHODS

The particular focus of this study is towards the integration of energy balance model with the GIS based groundwater flow model. At first the evapotranspiration and effective precipitation are determined by executing the computer scripts. These scripts are then linked with the database where all raw and processed data (point, raster) stores. The flow chart as shown in Figure 4 represents the preparation of input parameters and their utilization in the form of raster maps due to the interaction of database with the groundwater flow model. Depending on the size of study area (width, height) the whole raster is divided into the pixels of equal size by using computer programs. Each raster map has pixel resolution of 897 m and pixel width of 899 m and they are carefully aligned (skewness, scale, spatial reference and offset are kept same) to avoid any uncertainty during raster processing. Two dimensional (2-D) spatially distributed groundwater flow model. i.e. r.gwflow in GRASS software [19] is used to simulate groundwater flow. This modelling software takes all the inputs in the form of raster format and produces output of groundwater heads in the same format. All the required input raster files are prepared for groundwater recharge and groundwater abstraction considering the distribution of cropping information.

All the data in raw or processed form is stored in the database. Data is acquired by data acquisition system as well as generated by processes, data analysis tools and application programs. The database is constructed by using open source object-relational PostgreSQL [20] database system. Due to having native programing interface of PostgreSQL with Python programming language, the stored procedures are simulated. Furthermore, the spatial data in the database is handled by using PostGIS database extender. The stored data in the form tables in the PostgreSQL database has a specific format (numbers or raster files). The whole modelling system is divided into different modules. The parameters which are estimated in one module are used by other modules. Initially, the raw datasets are fetched from the comma separated values (CSV) file in to the PostgreSQL database tables. Overall, the setting of all raster maps in database is organized in such a way that, they can be fully processed and accepted by GIS-GRASS [21] database as shown in Table 2. For groundwater flow simulations in r.gwflow groundwater model, all raster maps need to be stored in the GIS-GRASS database.

Distributed Groundwater Recharge from Fields and Canals: The spatially distributed recharge from irrigation fields is estimated based on the information of actual evapotranspiration, effective precipitation and irrigation

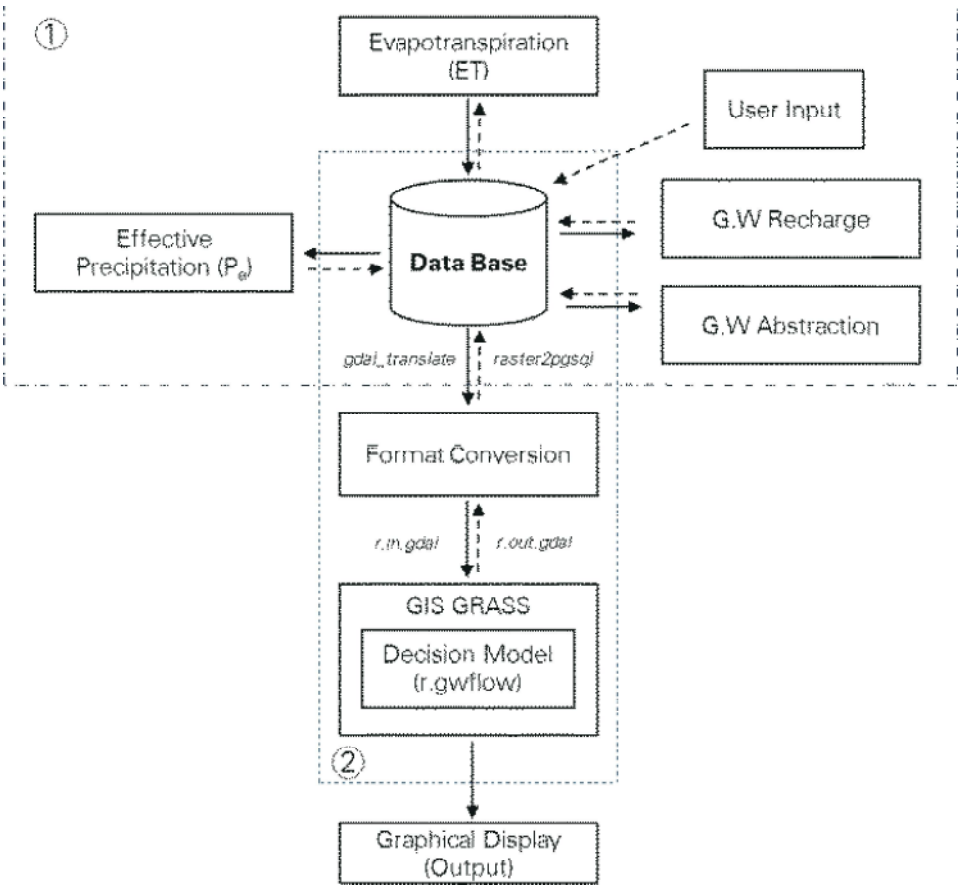

Fig. 4: Flow chart of developed modelling system

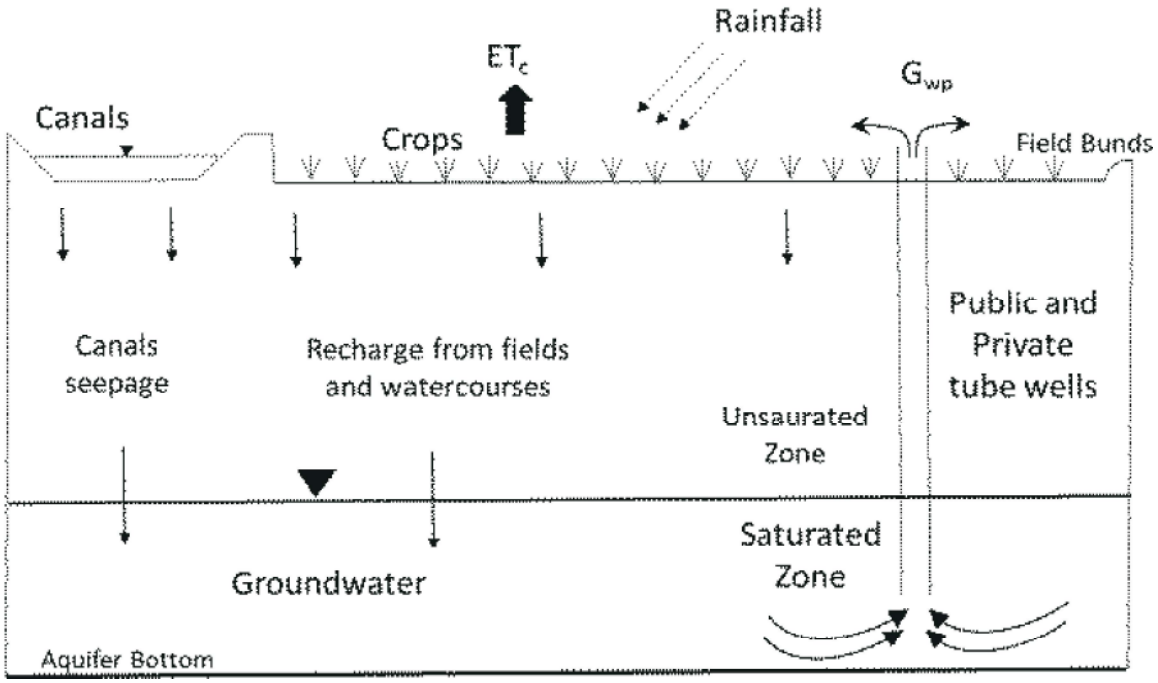

Fig. 5: Schematic diagram of water balance components

Table 2: Regional settings of GIS GRASS dataset.

Settings	Values
EPSG[1] Code	3857
North	3637673.680
South	3577583.630
West	8035600.160
East	8105713.797
Pixel height [m]	896.87
Pixel width [m]	898.89
Rows	67
Columns	78
Cells	5226

[1]EPSG is Spherical Mercator Projection Coordinate System

water application efficiency (E_a) by using the (Eq. 1) as suggested by [1]. The value of E_a is taken as a variable depending upon the type of crop grown in the study area [22, 23, 24, 25].

$$I_{FF} = \left[\frac{(ET_c - P_e) \times 100}{E_a} \right] \quad (1)$$

where, I_{FF} is the total irrigation water requirement at the field [mm month^{-1}].

The groundwater recharge from irrigation canals as a result of seepage is estimated by using (Eq. 2) [26]. The historical canal flow data and shape files of canal network are processed in GIS software for this purpose.

$$q_c = W_p . K_{soil} . \frac{(H_w + L_F - h_{we})}{L_f} \quad (2)$$

where, q_c is the seepage rate per meter length of channel [m^{2}s^{-1}], $W_p = W_b + \frac{2H_w}{\sin\alpha}$, is the wetted perimeter of the channel [m], W_b is the width of the channel base [m], H_w is the height of water in the channel [m], α is the angle at which channel sides meet the horizontal [rad], K_{soil} is the vertical saturated hydraulic conductivity of the soil [ms^{-1}], L_f is the thickness of the soil layer from the base of the channel [m], h_{we} is the negative pressure head at the base of the soil layer [m].

The reference evapotranspiration (ET_o) is estimated by using the Penman-Monteith method (Eq. 3) [3].

$$ET_0 = \frac{0.408\Delta(R_n - G) + \gamma \frac{900}{T + 273} \mu_2 (e_g - e_a)}{\Delta + \gamma(1 + 0.34\mu_2)} \quad (3)$$

where, ET_o is reference evapotranspiration [mm day^{-1}], R_n is net radiation at the crop surface [MJ m^{-2} day^{-1}], T is mean daily air temperature at 2 m height [°C], μ_2 is wind speed at 2m height [m s^{-1}], e_s is saturation vapour pressure [KP_a], e_a is actual vapour pressure [KP_a], e_s-e_a is saturation vapour pressure deficit [KP_a], ? is slope of vapour pressure curve [KP_a°C^{-1}], ?? is psychrometric constant [KP_a°C^{-1}].

To estimate the crop evapotranspiration (ET_c) by using (Eq. 4), the single crop coefficient approach is used. The crop coefficients (K_c) are based on local conditions for the crops grown during the rabi and kharif cropping season within the study area as shown in Figure 3.

$$ET_0 \times K_c = ET_c \quad (4)$$

The effective precipitation is estimated by using USDA-SCS method [27] as represented by (Eq. 5).

$$P_e = SF(0.70917 P_t^{0.82416} - 0.11556)(10^{0.02426 ET_c}) \quad (5)$$

$$SF = (0.531747 + 0.295164\, D - 0.057697\, D^2 + 0.003804\, D^3) \quad (6)$$

where, P_e is the average effective precipitation [mm], P_t is monthly mean precipitation [mm], SF is the soil water storage factor [--] as estimated by using (Eq. 6) [27], D is the usable soil water storage [mm] and is estimated by considering the maximum root depth [22] of crops in the study area.

Groundwater Abstraction: Due to the lack of data available about pumping wells, the utilization factor approach [17] for groundwater abstraction can not be utilized. However, it is estimated by using the indirect approach of water balance at farm level devised by [1].

$$G_{wp} = I_{FF} - I_{Canal} \quad (7)$$

where, G_{wp} is the groundwater abstraction [mm month^{-1}], I_{canal} is the canal water supply at agricultural farms [mm month^{-1}].

This approach is based on the fact that the crop water requirement in the agricultural fields is fulfilled by only two means, i.e. groundwater and canal water supply. I_{canal} is estimated by taking into account all the conveyance and seepage losses. In his way the groundwater pumping is determined by subtracting I_{canal} from I_{FF}.

Initial Piezometric Heads: Initial piezometric heads for the transient model are retrieved by interpolation of piezometric data using different interpolation techniques

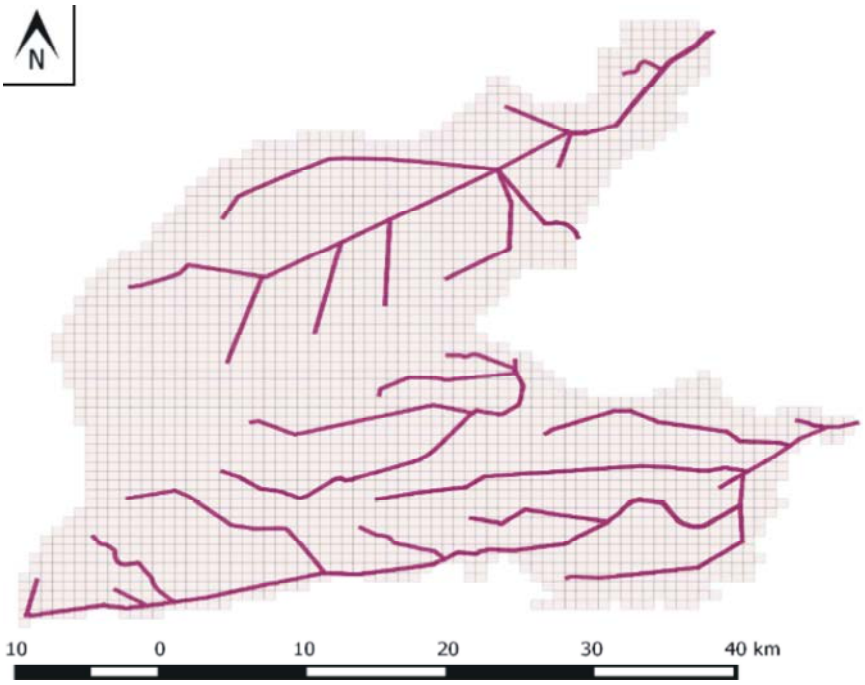

Fig. 6: Pixel based recharge from fields and canals

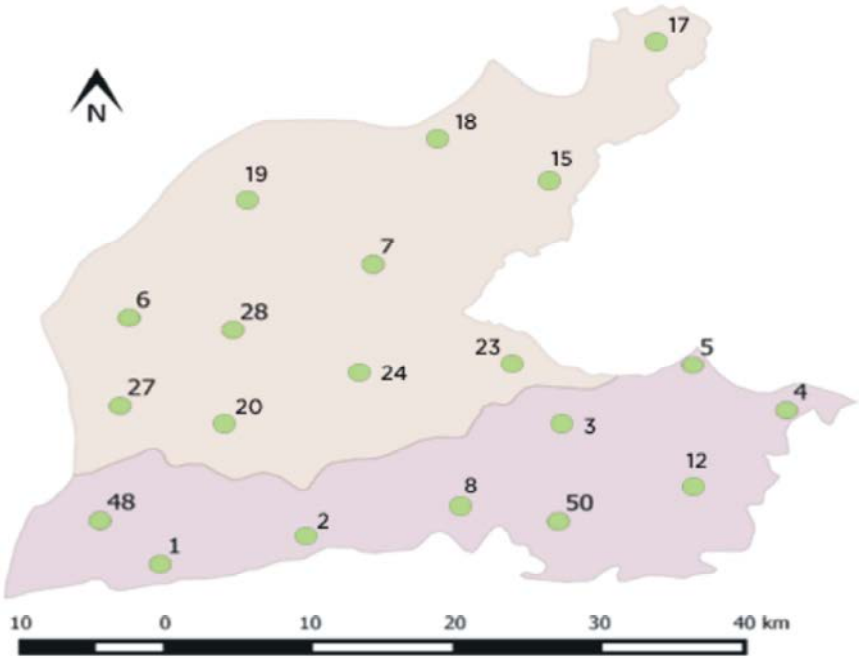

Fig. 7: Location of piezometers

(Inverse Distance Weighted (IDW), Bilinear, Cubic Convolution and Nearest Neighbor Method). When the produced surface maps are compared with the observed data taken from piezometers as shown in Figure 7, it is found that the nearest neighbor method is proved to be the most suitable to get groundwater maps.

Boundary Conditions: For each pixel in a raster map the boundary condition is defined by preparing a status map which contains three numbers, i.e., 0 for inactive pixels, 1 for Neumann type boundary condition and 2 for Dirichlet type boundary condition. On the western side of the study area, Trimmu Sidhnai (T.S) link canal flows as

shown in Figure 1 which transfers water from Chenab River to Ravi River. This link canal keeps running throughout the year with less variation in flow, therefore, the pixels of a raster map along this canal have a Dirichlet boundary condition. Along the southern boundary, Ravi River flows which originates from India and water levels are recorded at certain locations along the river. Time varying Dirichlet boundary condition was applied as conductance and other river geometry data was not available from any source. On the northern and eastern boundary of the model the Neumann type boundary condition is defined due the dependency of heads as a function of time and space. The remaining pixel present within the study area are active and have homogeneous Neumann boundary condition. These pixels contribute to the increase or decrease of piezometric head value due to recharge or pumping out of groundwater. The pixel outside the study area are inactive.

Hydraulic Conductivity/effective Porosity: Depending on the soil textural classes, hydraulic conductivity values were taken from [28] and effective porosity values were retrieved from [29] for all test boreholes by taking weighted average values. The spatially distributed maps of hydraulic conductivity and effective porosity were then generated through nearest neighbor interpolating technique.

Top/Bottom Surface: The digital elevation data of 90 m resolution were retrieved from http://srtm.csi.cgiar.org/ (CGIAR-CSI 2008) collected by Shuttle Radar Topography Mission (SRTM). Along with other model inputs in the form of raster maps the bottom depth of the study area is also described. As the bedrock in the study region is rarely known therefore it is decided to deduct 90 meter from the top surface to use as a bottom surface of 2-D model. The workflow of groundwater flow model (r.gwflow) is shown in Figure 8.

Calibration and Scenarios Simulation: The groundwater flow model is calibrated by using the measured water levels in the piezometers. Piezometric readings are generally taken bi-annually, once at the end of rabi season and other one at end of kharif season (i.e. post monsoon season). The hydraulic conductivity and porosity are adjusted manually until there is a least difference between measured and simulated values of piezometer heads. During the process, these values were kept in a range taken from [29] as well as [28] depending on each soil texture class. In the period of analysis (12 months) only two set of readings at piezometers were available which were collected on 15 October, 2010 and 15 April, 2011. The data collected on 15 October were used for calibration while data collected on 15 April, 2011 were utilized for validation of the model.

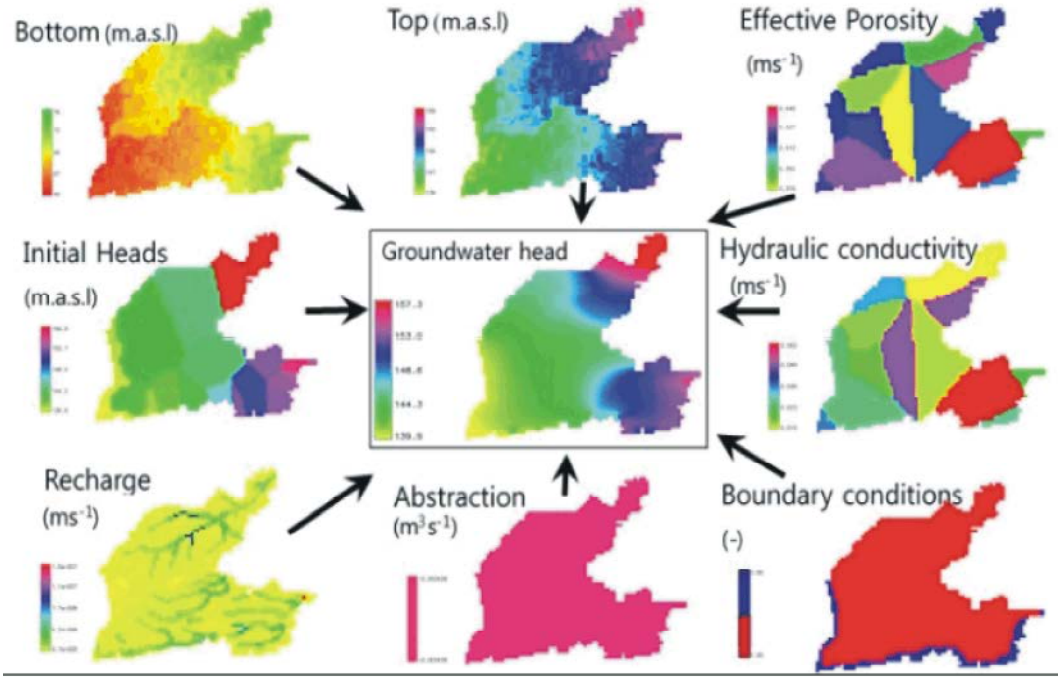

Fig. 8: Workflow of groundwater flow model (r.gwflow)

Table 3: Scenarios simulation under different irrigation system and cropping patterns in accordance with actual situation

	Cropping Pattern in Actual Situation				Cropping Patterns under Scenarios	
Scenarios	Kharif	Rabi	% increase	Ea (%)	Kharif	Rabi
1	Sugarcane (28%),	Sugarcane (17%),	0 (business as usual)	75	Rice (75%) and Fodder (21%)	Wheat (79%) and Fodder (17%)
2	Cotton (21%),	Wheat (47%),	0 (business as usual)	75	Cotton (75%) and Fodder (21%)	Wheat (79%) and Fodder (17%)
3	Barren (4%),	Barren (4%) and	0 (business as usual)	75	Sugarcane (96%)	Sugarcane (79%) and Fodder (17%)
4	Rice (26%) and	Fodder (32%)	30	85	Rice (75%) and Fodder (21%)	Wheat (79%) and Fodder (17%)
5	Fodder (21%)		30	85	Cotton (75%) and Fodder (21%)	Wheat (79%) and Fodder (17%)
6			30	85	Sugarcane (96%)	Sugarcane (79%) and Fodder (17%)
7			50	90	Rice (75%) and Fodder (21%)	Wheat (79%) and Fodder (17%)
8			50	90	Cotton (75%) and Fodder (21%)	Wheat (79%) and Fodder (17%)
9			50	90	Sugarcane (96%)	Sugarcane (79%) and Fodder (17%)

Model simulations under various scenarios were performed. Nine different scenarios are simulated by changing the cropping pattern, irrigation canal water supply (I_{canal}) and irrigation application efficiency $(E)_a$ considering the fact that these scenarios will affect the actual evapotranspiration, groundwater pumping rate, canal recharge and recharge from fields. The investigated scenarios have the significance that, they are not hypothetical but are based on actual agro-ecological conditions. Table 3 shows the seasonal crops cultivation in the study area and the scenarios simulation by the change in irrigation system parameters (I_{canal}, E_a) and seasonal cropping patterns.

Likewise, the cropping pattern scenarios are finalized by defining the percent area covered by each crop as shown in Table 3. The crop types are selected in such a way that their impact on groundwater levels can be fully analyzed due to recharge from fields and groundwater abstraction. Rice, wheat and cotton are considered as important crops and they fulfill major food requirements of the country. The area covered under these crops is taken larger as compared to fodder crops.

RESULTS AND DISCUSSION

The developed modelling system to simulate the groundwater flow in the study area consists of estimation of water balance components, model calibration, groundwater flow simulation and scenarios implementation.

Water Balance Components: In the study area, June and July are the hottest months of the year and the ETc increases from May to the highest point on June and then it starts decreasing before rising again at the end of winter (February). The ET_c also depends on the starting and ending time as well as on the length of the crop growing period. Initially the crops have less water requirement and then it increases with the growth period before reducing again at the last stage. From June to September there are also heavy moon soon rainfalls contributing to the large part of effective precipitation (Pe) as shown in Figure 9. The ET_o estimation through Penman-Montieth method is compared with the Blaney-Criddle method [3]. It is find out that Et_o values determined by using prior approach are more reliable. The estimated values of canal water supplies and actual evapotranspiration are shown in Table 4.

After analyzing the total crop water requirements, it is found from the canal discharge data that the water supplied by them is only 51% of total water requirement and the remaining is fulfilled by extracting the groundwater. The highest pumping rates are in the months of May and June because of the highest evapotranspiration, limited canal supply and starting of cultivation period of all crops at the same time (i.e. May). In the months of July and August, the groundwater abstraction was only 37.5 Mm^3 and zero because of torrential rainfalls (i.e. start of monsoon from mid July) despite having high crop water requirement. In the remaining months groundwater abstraction varied according to the crop water needs.

The monthly recharge values are shown in Figure 10 from different components of the irrigation system, i.e., from canals seepage and also the recharge from fields. Recharge rates from the fields depend on the total water requirement, effective precipitation and application efficiency of irrigation on farms. From the current study findings, total recharge is maximum during the months of May and June in which the water requirement is highest. It can be seen in Figure 10 that, the overall groundwater abstraction is more than groundwater recharge.

Calibration, Validation and System Characterization: The groundwater flow model incorporating all the water balance terms was calibrated using the measured values

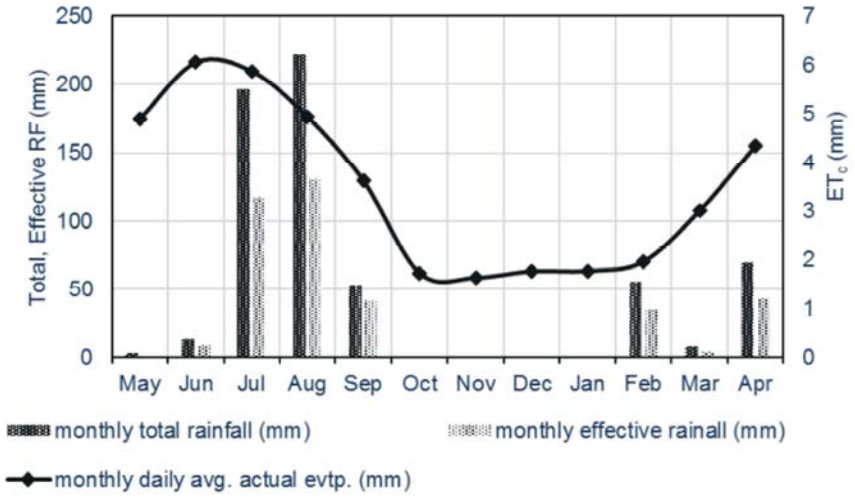

Fig. 9: Trends of total, effective rainfall and actual evapotranspiration (ET_c)

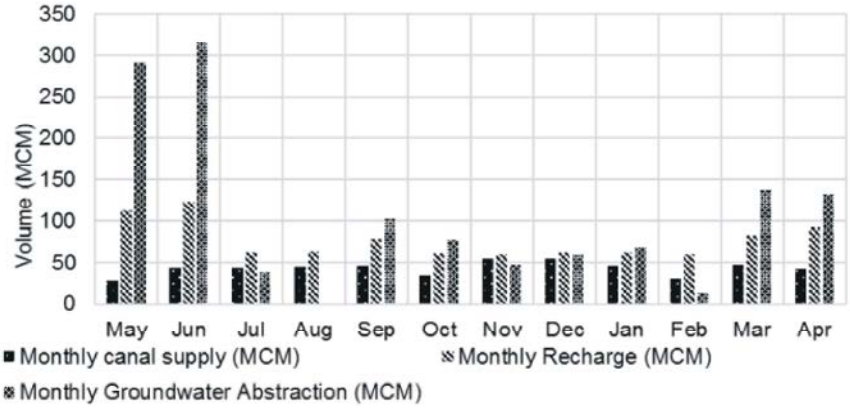

Fig. 10: Water budget in the study region.

Table 4: Canal water supplies and actual evapotranspiration within a simulation period.

Month	Canal Water Supply (mm day^{-1})	Actual Evapotranspiration (mm day^{-1})
May	1.6	1.8
Jun	0.9	2.0
Jul	1.7	3.3
Aug	1.4	3.3
Sep	0.6	4.9
Oct	1.7	6.1
Nov	1.8	5.9
Dec	1.5	4.9
Jan	1.7	3.6
Feb	1.4	1.7
Mar	1.9	1.6
Apr	1.9	1.8

Table 5: Hydraulic parameters after model calibration and validation

Parameters	Units	Value
Effective Porosity (p_e)	- -	0.375 - 0.44
Horizontal Hydraulic Conductivity (K_h)	ms^{-1}	0.0115 - 0.062
Vertical Hydraulic Conductivity (K_v)	ms^{-1}	0.00115 - 0.0062

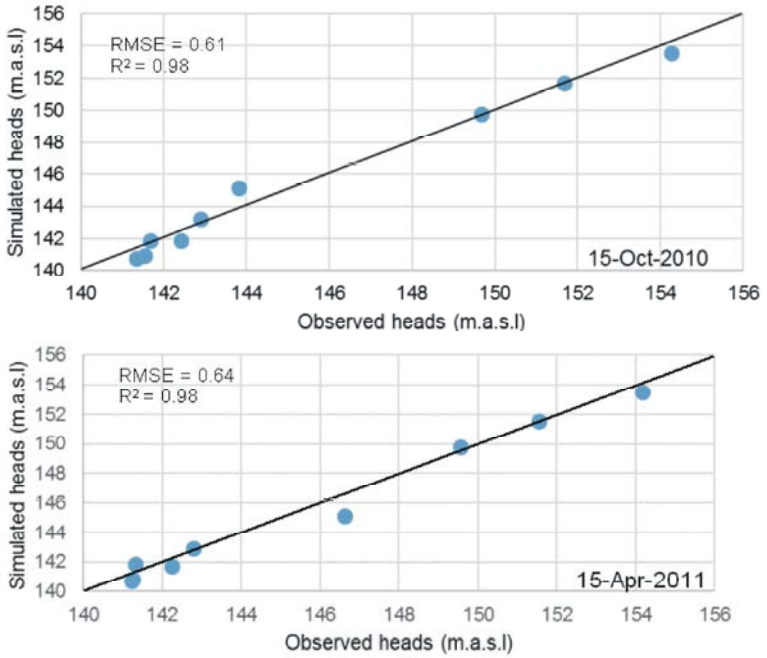

Fig. 11: Graphs between spatially distributed simulated and observed heads at two different time periods a) 15 October, 2010 b) 15 April, 2011.

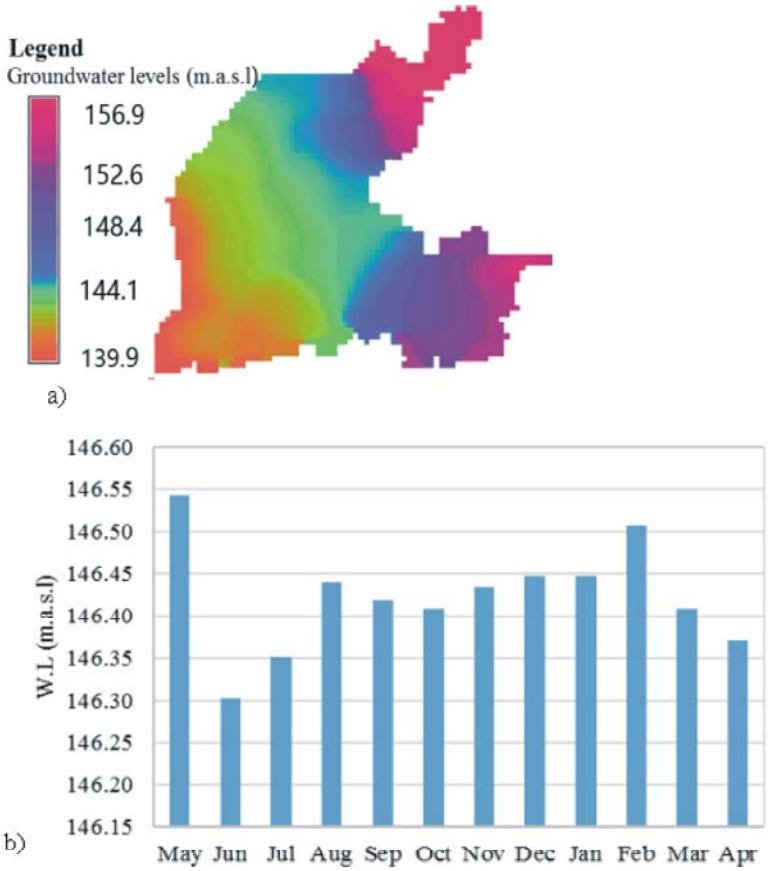

Fig. 12: (a) Raster map of simulated groundwater levels in May 2010, (b) Monthly averaged water levels of the study area

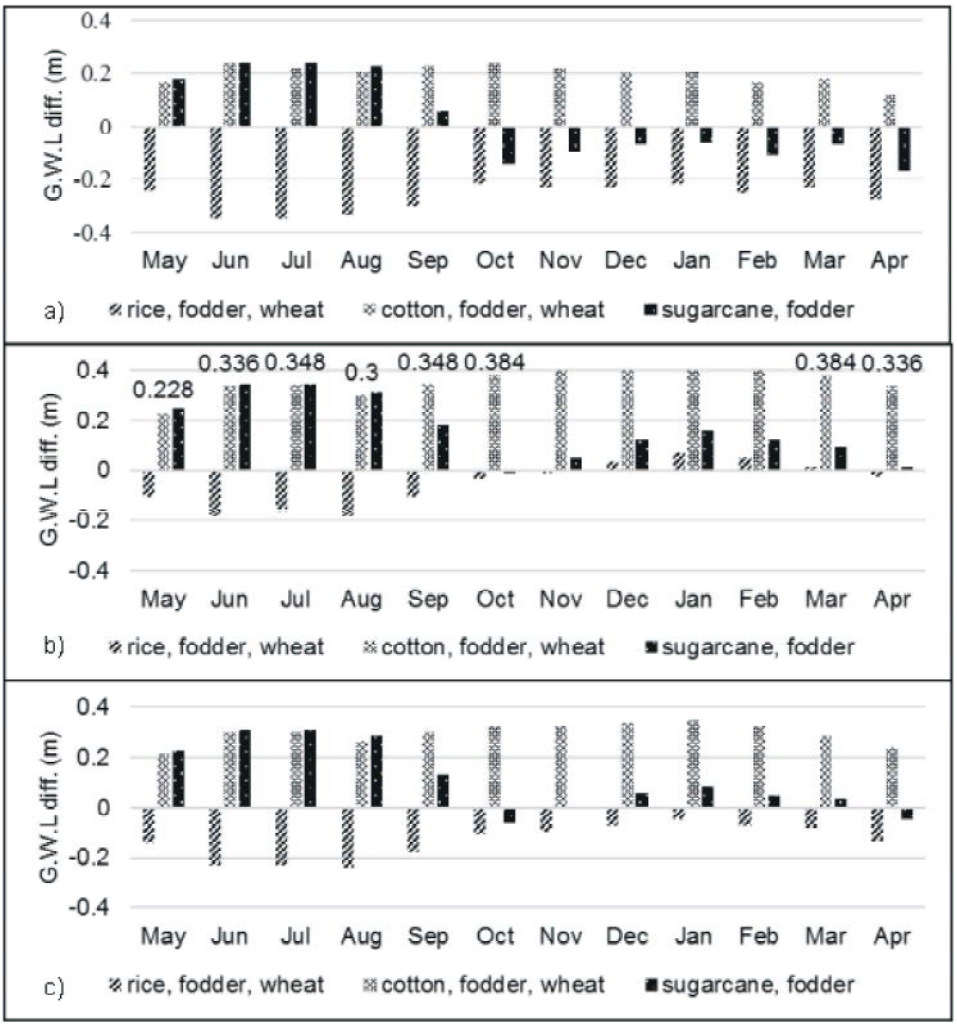

Fig. 13: Groundwater level variations in (a) scenarios 1 to 3 (b) scenarios 4 to 6 (c) scenarios 7 to 9

through iteration process. The hit and trial procedure was adopted for parameter adjustment at each time for all observation points. For calibration, the measured heads on 15 October, 2010 were used. After calibration, the model was rerun to check the difference between measured and simulated groundwater levels for piezometric data collected on 15 April, 2011 as shown in Figure 11.

The root-mean-square error (RMSE) for the observed and simulated piezometer heads for calibration is found to be 0.61 whereas, the value of RMSE for validation is is 0.64. The co-efficient of determination (R^2) values for both calibration and validation of model are found to 0.98. The hydraulic parameters obtained after model calibration and validation are shown in Table 5.

The raster maps for each month of the simulation period representing the groundwater levels are produced. For instance, figure 12a is the output raster map for the month of May and the monthly average water levels are shown in Figure 12b. It is observed that majority piezometers showed increasing trends in groundwater level which is mainly associated to heavy monsoon rainfalls in the months of July and August. Similarly, in the month of February, there is again a rise in water level which is due to winter rainfall in the month of February. Rabi season (i.e. November - April) showed overall drop in groundwater levels except February, but the drop was comparatively less as compared to kharif season. Similar kind of trends can be seen in the monthly averaged groundwater levels for the study area.

Scenarios Simulations: The response of groundwater flow is analyzed by implementing the developed system for different cropping patterns under different irrigation regimes. This activity helps in the future planning and devising strategies under suitable combination of crops

among all the scenarios by finding out the dynamics in groundwater levels. The average simulated groundwater levels under different scenarios are compared with the averaged simulated groundwater levels at current times which are also considered as reference. The difference between the monthly referenced groundwater levels and monthly averaged groundwater levels for different scenarios are worked out and presented in figure 13. Nine different scenarios are simulated by taking three different crop combinations (both for rabi and kharif cropping seasons) and three types of variations in different irrigation system parameters related to canal water supply and application efficiency. The summary of these different scenarios are presented in the chronological order below.

In the scenarios 1 to 3, the simulations are performed by taking I_{canal} and E_a as a business as usual (actual situation) with different crops combination and the results are shown in Figure 13a. The first scenario containing cropping pattern with sugarcane (96%) and remaining area with barren or fallow shows higher groundwater levels in kharif season than the reference. However, in the rabi season, the groundwater levels with cropping pattern containing sugarcane (79%) and fodder (17%) are decreasing below than the reference. The rise in groundwater levels is observed in the months of June and July, i.e. 0.24 m, while its drop is witnessed in the months of October and April up to -0.144 m and -0.168 m, respectively. In contrast to first scenario, the second scenario (i.e., 75% cotton, 21% fodder, in kharif season and 79% wheat, 17% fodder, in the rabi season) shows rise in groundwater levels throughout the simulation period. This scenario shows the maximum and minimum rise in groundwater level during the period from September to October with a value of 0.24 m and 0.12 m in the month of April, respectively. The entirely different groundwater trend is observed for the third scenario (i.e., 75% rice, 21% fodder during kharif and 79% wheat, 17% fodder during rabi), where groundwater levels drop in comparison to reference condition due to higher crop water demands. During kharif season, maximum groundwater drop can be visualized during periods from June to August i.e. -0.35 m, while in rabi it is observed in April with a value of -0.28 m.

For the scenarios from 4 to 6, I_{canal} and E_a are increased by 30% and 10% along with different cropping patterns and the results are shown in figure 13b. In these all scenarios (4 to 6) there is an increase in groundwater levels in contrast to groundwater levels for scenarios 1 to 3. The fourth scenario which contains sugarcane and fodder in both kharif and rabi seasons shows maximum increase in groundwater levels reaching up to 0.35 m during the months of June to July. Nevertheless, at the end of kharif season the groundwater levels under the scenario 4 is similar to reference condition. For the fifth scenario (i.e. with cotton, fodder and wheat crops), the groundwater levels show major gains (in levels) for both seasons (i.e. kharif and rabi). The maximum rise is observed in the kharif season during the months from July to September with a value of 0.35 m, whereas during the rabi season, the highest increase is 0.46 m, which can be visualized in the month of January. The trend of groundwater is found negative for the sixth scenario (i.e. with rice, fodder and wheat crops) during the entire kharif season with a highest fall of -0.18 m is in the months from June to August. During the entire rabi season, there is a slight increase in the groundwater levels (maximum of 0.07 m in the month of January), excluding April with a decline of 0.024 m.

Correspondingly, the simulated groundwater responses under different scenarios from 7 to 9 are shown in figure 13c. In these scenarios I_{canal} is increased to 50% and E_a is taken as 90% which is 15% more than the reference. In contrast to the scenarios from 4 to 6, the groundwater levels in these scenarios (7 to 9) are relatively lower. The reason for these lower groundwater levels is the reduction in groundwater recharge from agricultural fields (i.e. 5% less than the scenarios from 4 to 6) due to increase in E_a (i.e. 90%). For the eight scenario under cotton, fodder and wheat crops, the highest groundwater increase is 0.35 m in January. Conversely, there is a decline of -0.24 m in August under scenario 9 containing rice, fodder and wheat crops under cultivation.

It can be concluded from the results of different scenarios that the cropping pattern containing combination of cotton, fodder and wheat is more suitable to develop groundwater. This combination of crops exhibit least differences in groundwater abstraction and recharge for different combinations of I_{canal} and E_a increase as shown in Figure 13. It is also found that under cotton, fodder and wheat cropping, the highest groundwater levels are observed for second scenario with a maximum value of 0.24 m, 0.46 m for fifth scenario and 0.35 m for eighth scenario. Under this aforementioned (i.e. most suitable) crop combination, the smoother trend with relatively low fluctuation of groundwater levels are achieved. The maximum fluctuations are 0.07 m in second scenario, 0.11 m in fifth scenario, 0.08 m in eighth scenario from May to June).

CONCLUSION AND RECOMMENDATIONS

The developed modelling system has the capacity to implement different cropping patterns and system parameters in such a way that optimum solution can be find out for decision making and planning. The modelling structure is flexible for changes and ready to connect with web application and further extensions. The main conclusions drawn from the study and outlook for future research and policy intervention are as follows:

- Groundwater simulations has confirmed the overall groundwater depletion and exploitation with time, however this decreasing trend is spatially varied. The water supplied by artificial irrigation canals fulfils only 51% of the total water requirement.
- Maximum groundwater pumping is in the months of May (290.46 Mm^3) and June (316.04 Mm^3). The maximum groundwater recharges, i.e., 112.26 Mm^3 and 123.27 Mm^3 are also in these two months.
- Increase in water application efficiency reduces both the groundwater abstraction and recharge in the fields. The increase in canal water supply helps in reducing groundwater abstraction but recharge from unlined channels increases as a result of rise in water heads.
- Cropping pattern containing crops of cotton, fodder (millet) in kharif season and wheat, fodder (barley, oat) in Rabi season is the most suitable combination for cultivation in the study area to avoid groundwater exploitation under current situation.
- The methodology of current study and the developed tool is a good start point to effectively manage the agricultural water use. However, the developed modelling system should be implemented on such an area where long term observed piezometric heads on monthly basis and with proper information related to groundwater abstraction (number of wells, pumping rate, operating hours etc.) is available, along with the metrological data.
- Besides considering only groundwater response, it is suggested that optimum cropping pattern should also be determined based on other single objective models, i.e. a) maximum net profit from the crops, b) maximum water use effectiveness, c) reduction in salinity load. Furthermore, the multi-objective model objective function can be made which considers all the single objective models by assigning different weights (priorities). Finally, the optimum cropping pattern can be selected based on the compromise between single objective models.

ACKNOWLEDGEMENT

The authors are really thankful to Association of Friends and Sponsors of TU Dresden e.V. Germany for providing funding for this study. Also, all the institutions which provided necessary data for accomplishment of this task are gratefully acknowledged.

REFERENCES

1. Usman, M., R. Liedl and A. Kavousi, 2015. Estimation of distributed seasonal net recharge by modern satellite data in irrigated agricultural regions of Pakistan. Environmental Earth Sci., 74(2): 1463-1486. doi:10.1007/s12665-015-4139-7.
2. Zbigniew, W.K. and D. Petra, 2009. Will groundwater ease freshwater stress under climate change?, Hydrological Sciences Journal, 54(4): 665-675, DOI: 10.1623/hysj.54.4.665.
3. Allen, R.G., L.S. Pereira, D. Raes and M. Smith, 1998. Crop Evapotranspiration- Guidelines for Computing Crop Water Requirements. Rome: FAO Irrigation and Drainage Paper 56.
4. Usman, M., R. Liedl and M. Shahid, 2014. Managing irrigation water by yield and water productivity assessment of a Rice-Wheat system using remote sensing. Journal of Irrigation and Drainage Engineering 2014 140: 7.
5. Er-Raki, S., A. Chehbouni and B. Duchemin, 2001. Combining satellite remote sensing data with FAO-56 dual approach for water use mapping in irrigated Wheat fields of a semi-arid region. Remote Sensing, pp: 375-386.
6. Szilagyi, 2013. Modis-Aided water-balance investigations in the republican river basin, USA. Periodica Polytechnica, Civil Engineering, pp: 33-46.
7. Szilagyi, J. and A. Kovacs, 2010. Complementary-relationship-based evapotranspiration mapping (cremap) technique for Hungry. Periodica Polytechnica, pp: 95-100.
8. Baalousha, H., 2005. Using CRD method for quantification of groundwater recharges in the GAza Strip, Palestine. Environ Geol., pp: 889-900.
9. Nolan, B.T., R.W. Healy, P.E. Taber, K. Perkins, K.J. Hitt and D.M. Wolock, 2006. Factors influencing ground-water recharge in the eastern United States. Journal of Hydrology, pp: 187-205.
10. Arshad, M. and M.R. Choudhry, 2005. Estimation of groundwater recharge from irrigated fields using analytical approach. International Journal of Agriculture and Biology, pp: 285-297.

11. Arshad, M., N. Ahmad and M. Usman, 2009. Simulating seepage from branch canal under crop, land and water relationships. International Journal of Agriculture and Biology, 11(5): 530-534.
12. Koradiya, K.A. and R.B. Khasiya, 2014. Estimate seepage losses in irrigation canal system. Indian Journal of Applied Research, 4(5).
13. Mowafy, M.H., 2001. Seepage losses in Ismailia canal. Sixth International Water Technology Conference, IWTC, Alexandria, Egypt pp 195-211.
14. Kalsoom, U., M. Arshad, S. Iqbal, M. Usman and M. Adnan, 2012. Use of GIS for the performance evaluation of canal irrigation in Rice wheat cropping zone. World Academy of Science, Engineering and Technology, pp 398-408.
15. Liu, W.C., 2004. Decision support system for managing ground water resources in the Choushui River Alluvial in Taiwan. Journal of the American Water Resources Association, pp: 431-442.
16. Stansbury, J., W. Woldt and I. Bogardi, 1991. Decision support system for water transfer evaluation. Water Resources Res., 27(4): 443-451.
17. Sarwar, A. and H. Eggers, 2006. Development of a conjunctive use model to evaluate alternative management options for surface and groundwater resources. Hydrogeology Journal, pp: 1676-1687. doi:10.1007/s10040-006-0066-8.
18. Khan, M.A., 1978. Hydrological data, Rechna Doab: lithology, mechanical analysis and water quality data of testholes/test wells. Vol. 1(25). Lahore: Project Planning Organisation-Pakistan Water and Power Development Authority (WAPDA).
19. Gebbert, S., 2013. r.gwflow. 06 15. https://grass.osgeo.org/grass71/manuals/r.gwflow.html. Accessed 10 September, 2015.
20. Postgre, S.Q.L., 2016. The PostgreSQL Global Development Group. https://www.postgresql.org/. Accessed 26 October, 2016.
21. GIS-GRASS, 2016. Bringing advanced geospatial technologies to the world (OSGeo Project). https://grass.osgeo.org/. Accessed 26 September, 2016.
22. FAO, 2012. Pakistan-Water report 37. http://www.fao.org/nr/water/aquastat/countries_regions/pak/index.stm. Accessed 21 August, 2015.
23. Jalota, S.K. and V.K. Arora, 2002. Model-based assessment of water balance components under different cropping systems in North–West India. Agric Water Manag, pp: 57: 75-87.
24. Tyagi, N.K., D.K. Sharma and SK. Luthra, 2000a. Determination of evapotranspiration and crop coefficients of rice and sunflower. Agric, Water Manag., 45: 41-54.
25. Tyagi, N.K., D.K. Sharma and S.K. Luthra, 2000b. Evapotranspiration and crop coefficients of wheat and sorghum. J. Irrig. Drain. Eng., 126: 215-222.
26. Morgan, L., G. Green and C. Wood, 2011. Simple analytic methods for estimating channel seepage from constructed channels in the Upper South East of South Australia. Adelaide: Department of Water-Technical Note 2011/04.
27. Martin, D.L. and J.R. Gilley, 1993. Irrigation Water Requirements. Chapter 2 of the SCS National Engineering Handbook Part 623. Washington D.C.: Soil Conservation Service. ftp://ftp.wcc.nrcs.usda.gov/wntsc/waterMgt/irrigation/NEH15/ch2.pdf. Accessed 26 September, 2016.
28. Freeze, R.A. and J.A. Cherry, 1978. Groundwater. USA: Englewood Cliffs, NJ 07632: Prentice-Hall.
29. McWhorter, D.B. and D.K. Sunada, 1977. Grounud-water hydrology and hydraulics. Fort Collins, Colorado: Water Resources Publications, LCC.